

Impact of variability and anisotropy in the correlation decay distance for precipitation spatial interpolation in China

Yingxian Zhang^{1,*}, Jose Hidalgo², David Parker²

¹Laboratory for Climate Studies, National Climate Center, China Meteorological Administration, Beijing 100081, PR China

²Formerly of Met Office Hadley Centre, Exeter EX1 3PB, UK

ABSTRACT: Correlation decay distance (CDD) plays a key role in the angular-distance weighting (ADW) interpolation technique, where it is used as the search radius to select correlated neighbors and to calculate relative weights. The purpose of this study was to assess any improvement obtained by using a regionally and seasonally variable CDD rather than a fixed CDD based on the entire mainland China daily precipitation dataset or the intermediate case of a seasonally invariant CDD within each region. We also assessed the influence of using anisotropic versus isotropic CDDs. We found that the CDD of daily precipitation in China varies spatially and seasonally, and it presents anisotropic behavior, as a result of topography and the predominant atmospheric circulation. In general, CDD is largest in winter and smallest in summer, except for limited regions such as the Tibetan plateau. From a cross-validation analysis, we found that taking account of spatial and seasonal variations in CDD generally improves ADW interpolation. Utilization of anisotropic CDDs increases the interpolation skill scores in regions with a dense monitoring network, significant elevation variation (southwestern China), or strongly anisotropic CDDs (Tibetan plateau).

KEY WORDS: Daily precipitation · Correlation decay distance · Angular-distance weighting interpolation

— Resale or republication not permitted without written consent of the publisher —

1. INTRODUCTION

One of the most common methods used to interpolate irregular observations to a regular grid is angular-distance weighting (ADW). ADW was originally developed by Shepard (Shepard 1968, 1984, Willmott et al. 1985). It includes an ‘angular’ term which accounts for the directional separation as seen from a target grid point, so that over-weighting of information from a densely sampled direction is avoided (Efthymiadis et al. 2006). All forms of ADW have a common approach that an estimate at a regular point is a weighted average of nearby irregular stations’ data, where individual station weight is a function of inverse distance from the point to be esti-

mated and angular isolation from other data points (Shepard 1968, Willmott et al. 1985, New et al. 2000, Hofstra & New 2009).

On global and regional scales, ADW has been used to create grid datasets of climatology (Legates & Willmott 1990a,b), monthly anomalies (New et al. 2000), daily series (Hofstra & New 2009, Herrera et al. 2012), and extreme indices (Kiktev et al. 2003, Alexander et al. 2006, Yin et al. 2015). For long-term gauge-based daily precipitation datasets in China, many interpolation methods have been used, such as thin-plate spline (Yuan et al. 2015) and optimal interpolation (Xie et al. 2007, Shen et al. 2010, Shen & Xiong 2016). Application of interpolation algorithms to extremes has taken 2 approaches: either calculat-

*Corresponding author: zhangyingxian@cma.gov.cn

ing indices then gridding (Yin et al. 2015), or deriving extreme indices from gridded datasets (Zhou et al. 2016). Differences in estimated extreme index trends between these 2 methods tend to be small, but differences in magnitudes are large.

The implementation of ADW often uses the concept of correlation decay distance (CDD), also called correlation length scale. CDD is used to guide the choice of which stations influence a grid value and to form the inverse-distance component of station weight. CDD is defined as the distance at which the correlation between one station and all other stations decays below e^{-1} (Briffa & Jones 1993, Jones et al. 1997, Hofstra & New 2009). When interpolating climate variables, the CDD has often been assumed to be isotropic (e.g. New et al. 2000). However, CDD can be anisotropic both for temperature (Jones et al. 1997) and precipitation (Hofstra & New 2009); daily climate series (Hofstra & New 2009) and extreme climate indices (Alexander et al. 2006); and global (Jones et al. 1997) and regional scales (Hofstra & New 2009). Using CDDs that varied spatially by seasonal or synoptic state would yield small improvements in ADW interpolation skill, relative to using a fixed CDD across the whole of Europe (Hofstra & New 2009). In other words, accounting for local conditions could improve the statistical performance of global measures. For instance, when the inverse-distance weighting method is adjusted for local sampling density, the results are superior to the standard results (Lu & Wong 2008). When regression is adjusted for local variability, local regressions always perform better than the global regressions (e.g. Brunsdon et al. 1998).

The purpose of this study is to assess any improvement obtained by using a regionally and seasonally variable CDD rather than a fixed CDD based on the entire mainland China daily precipitation dataset or the intermediate case of a seasonally invariant CDD within each region. We also assess the influence of using anisotropic versus isotropic CDDs. Before interpolating, we applied a bias correction to daily precipitation data from each gauge in terms of wind-induced undercatch, wetting losses, and neglect of trace precipitation amounts in order to improve the accuracy and systematic biases in the precipitation data series.

Formal explanations about CDD and the ADW interpolation technique are presented in Section 2. In Section 3, the daily precipitation dataset and bias-correction method are introduced. Section 4 presents the spatial and seasonal variability in CDD and its spatial field of anisotropy for precipitation. In Section 5, we use different CDDs along with one year (2008)

cross-validation to test the sensitivity of ADW interpolation skill to the assumptions about CDD, and suggest the best choice of CDD in each region of mainland China for precipitation spatial interpolation. In the last section, some conclusions are listed.

2. CDD AND ADW INTERPOLATION TECHNIQUE

CDD is the key component for the ADW interpolation technique, which is usually calculated as follows. First, Pearson correlation coefficients between the target station and each other station are determined. Then these values are sorted by spherical-geometry distance (Willmott et al. 1985) to the target station and an exponential function is fitted by least squares to the cloud of points. The CDD is set as the distance where the fitted exponential function is equal to e^{-1} . Relatively short CDDs indicate that only nearby stations within this distance have a significant correlation, whereas a larger CDD arises when more distant stations are also significantly correlated with the target point (Briffa & Jones 1993, Jones et al. 1997, Osborn & Hulme 1997, Hofstra & New 2009).

The weights of ADW interpolation include 2 components: the distance term and the angular term, which accounts for the geographical separation of the sites of the time series. This technique relies on the fact that the inter-relation of stations decreases with distance, both in terms of the time-mean and the variability. Thus in terms of local averaging, it is reasonable to assign higher weights to nearby-located stations than to remote ones. Moreover, since the time series averaged are, in general, unevenly distributed in space, the angular separation between the sites of the interpolated time series is taken into account by avoiding over-weighting of information from the same sector: well-separated stations are more strongly weighted than nearby ones (Efthymiadis et al. 2006). The angular distance weight for each station i is the outcome of their product (Hofstra & New 2009):

$$w(i) = w_{\text{rad}}(i) \times w_{\text{ang}}(i) \quad (1)$$

where w is the integrated weight, w_{rad} is the distance weight, and w_{ang} is the angular weight. All stations within the search radius (which equals CDD) from the target grid for interpolation are selected. The distance term $w_{\text{rad}}(i)$ assigned to each station i is an exponential function of its distance x from the target grid point:

$$w_{\text{rad}}(i) = (e^{-x/\text{CDD}})^m \quad (2)$$

where m is a constant global parameter, and setting to 4 is an optimal performance after cross-validation. This value has also been used by New et al. (2000) and Hofstra & New (2009). The angular term for each station is:

$$w_{\text{ang}}(i) = 1 + \frac{\sum_{k=1}^n w_{\text{rad}}(k)[1 - \cos\theta_{ki}]}{\sum_{k=1}^n w_{\text{rad}}(k)}, i \neq k \quad (3)$$

where n is the number of contributing stations within the CDD, and θ_{ki} is the angular separation of stations k and i with the vertex of angle defined at the target grid point. The overall weighting favors stations closest to the target grid or more isolated.

3. DATASET

3.1. Observations

We use daily precipitation from a dense national network of ~2400 gauges (Fig. 1a) from 1951 to 2013 provided by the National Meteorological Information Centre (NMIC) of the China Meteorological Admin-

istration (CMA). All the data had been subject to quality control by NMIC, including extreme checks and internal consistency checks. There are 115 breakpoints from 35 gauges, and the proportion of inhomogeneous gauges is about 1.46 % (Shen & Xiong 2016). Breakpoints are the abrupt shifts in climate time series due to natural and artificial reasons. Usually, artificial breakpoints are introduced by changes in measurement conditions, relocation of weather stations, land-use changes, new instrumentation or changes in observational hours, among others, which are sometimes recorded in the metadata (Kuglitsch et al. 2009). Climate time series with no breakpoints are homogeneous. Owing to the complexity of daily precipitation precluding the availability of highly correlated reference series, along with the lack of original metadata, inhomogeneous rainfall series have not been corrected. In addition, excluding all the inhomogeneous gauges would likely remove some real records, and it is quite difficult to determine the causes of inhomogeneity, due to the lack of supporting metadata. Therefore, the inhomogeneous gauges were included in our work.

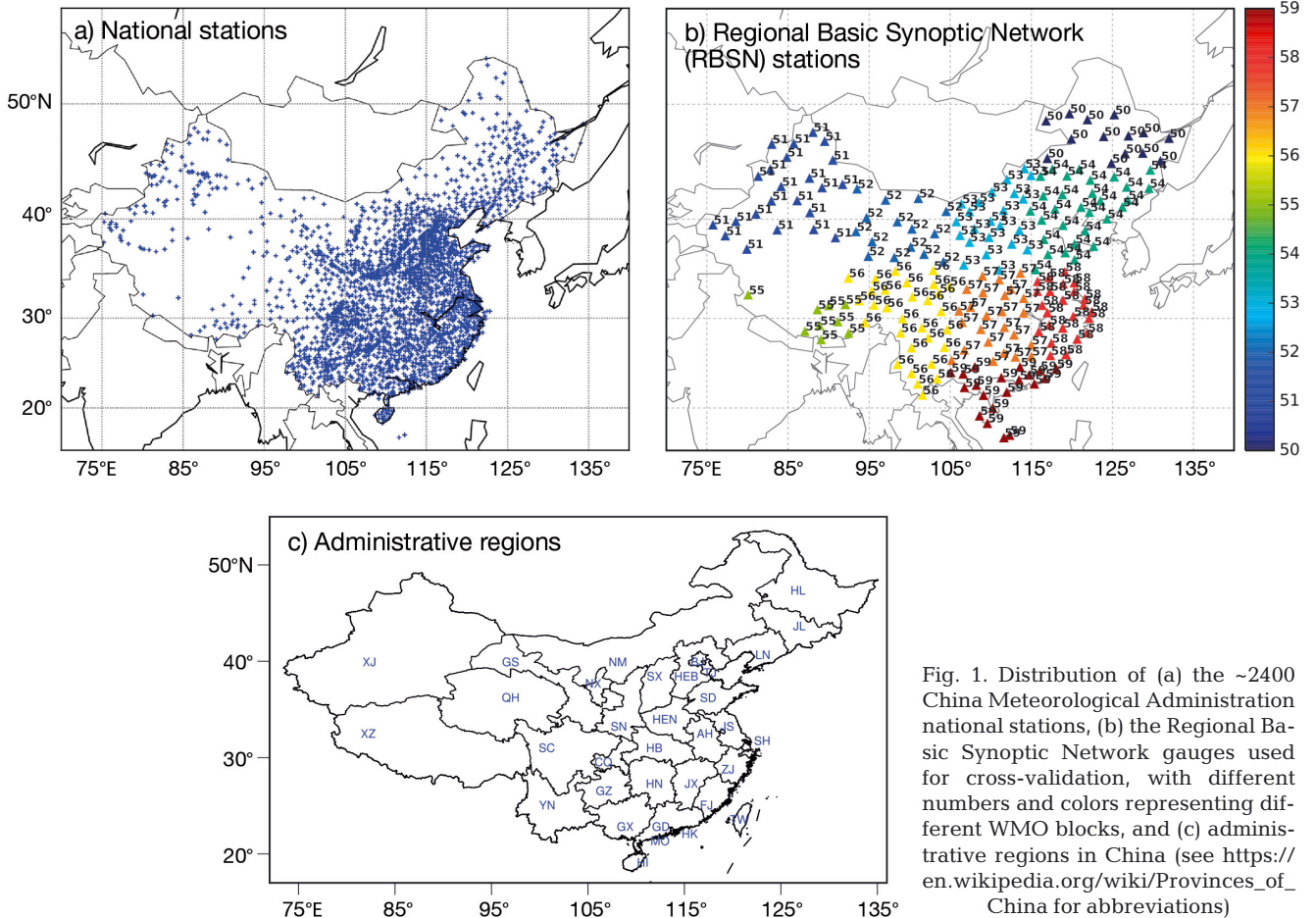


Fig. 1. Distribution of (a) the ~2400 China Meteorological Administration national stations, (b) the Regional Basic Synoptic Network gauges used for cross-validation, with different numbers and colors representing different WMO blocks, and (c) administrative regions in China (see https://en.wikipedia.org/wiki/Provinces_of_China for abbreviations)

Fig. 1a indicates that the network of gauges is dense in southern and southeastern parts of China, while it is sparse in the northern and north-western parts. Fig. 1b shows 213 gauges of the Regional Basic Synoptic Network (RBSN), which belongs to ~2400 CMA gauges and has an even distribution across the whole of China. We plan to use these RBSN stations for cross-validation. There are a total of 34 administrative regions in China (Fig. 1c), some of which we use in Section 4.2 to show geographical variations in CDD. Fig. 2 shows the number of available stations year by year with different thresholds for at least 75, 90, and 99% valid daily records within each year. We found that the number of stations grows until 1961, where it remains >2000. This poses some limitations for a trend analysis before 1961. There are >60 gauges with incomplete records in the period of 1968, and most gauges have >2 months missing. Unfortunately, the reason is still unclear at present. Therefore, there is a small dip in the number of valid stations in 1968 in Fig. 2.

3.2. Bias correction

It has been recognized that uncertainties exist in regional (Ye et al. 2004) and global precipitation climatology (Korzun et al. 1978, Goodison et al. 1998) due to biases of gauge measurements such as wind-induced gauge undercatch (Yang et al. 2001), wetting and evaporation losses, and neglect of trace precipitation amounts. Wetting losses are due to precipitation retaining or sticking to the sides of the gauge which cannot be poured out and measured (Ye et al. 2004). A precipitation event of <0.1 mm is recorded as a trace amount of precipitation in China. It is unreasonable for trace events to be treated as precipitation days, so they are treated as zero amounts quantitatively. Wind-induced undercatch is caused by wind field deformation over the gauge orifice (Sevruk & Hamon 1984, Ye et al. 2004). Though this correction is a complicated issue, it is necessary to undertake. These systematic errors in gauge measurements should be corrected, because these biases may be substantial, especially in cold environments (Ye et al. 2004). Wind-induced gauge undercatch is the greatest bias in most regions of mainland

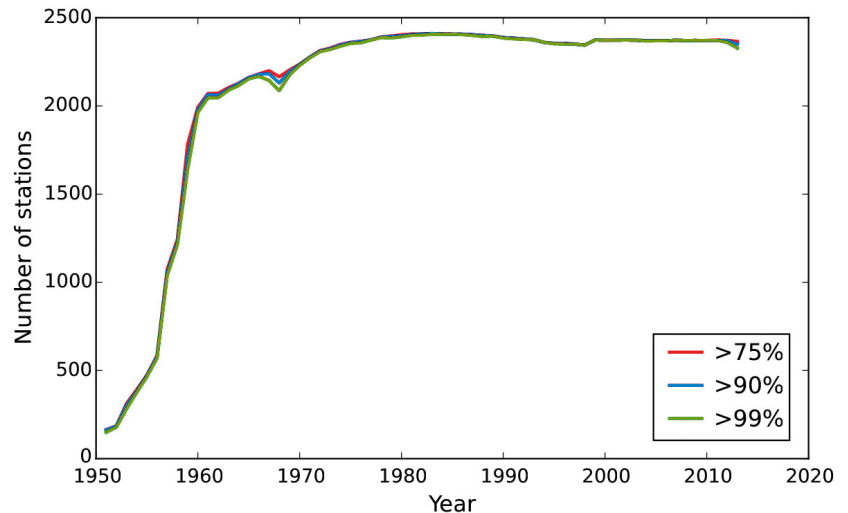


Fig. 2. Temporal evolution of the number of available stations with at least 75, 90, and 99% valid daily records within each particular year

China (Ye et al. 2004). The effect of wind-induced error on the estimates of winter snowfall trends is particularly significant in northeastern China, with a maximum overestimate for measured long-term trends reaching 1 mm every 10 yr, or approximately 64.3% in terms of relative bias between measured and corrected trends (Sun et al. 2013). Wetting loss and neglect of trace amounts of precipitation are more important in the arid and semi-arid regions of China than in the wet regions (Ye et al. 2004).

Therefore, before interpolation, a bias-correction methodology developed by Ye et al. (2004) was applied to daily data for ~2400 observation sites in China during 1951–2013 to improve the accuracy of precipitation data and systematic biases in the precipitation data series. According to Ye et al. (2004), the general model for precipitation correction is as follows:

$$P_c = K(P_g + \Delta P_w + \Delta P_e + \Delta P_t) \quad (4)$$

where P_c is the corrected precipitation; P_g is the gauge-measured precipitation; ΔP_w and ΔP_e are wetting loss and evaporation loss, respectively; ΔP_t is the trace precipitation; and K is the correction coefficient for wind-induced errors.

To determine the systematic biases in Chinese gauge measurements, a gauge intercomparison study was carried out during 1985–91 at 4 meteorological stations in the Urumqi River basin, and the methodology was developed to determine each item in Eq. (4) (above, by Yang 1988 and Yang et al. 1991). Using only 4 stations to estimate bias seems like not enough to give a comprehensive estimate across the

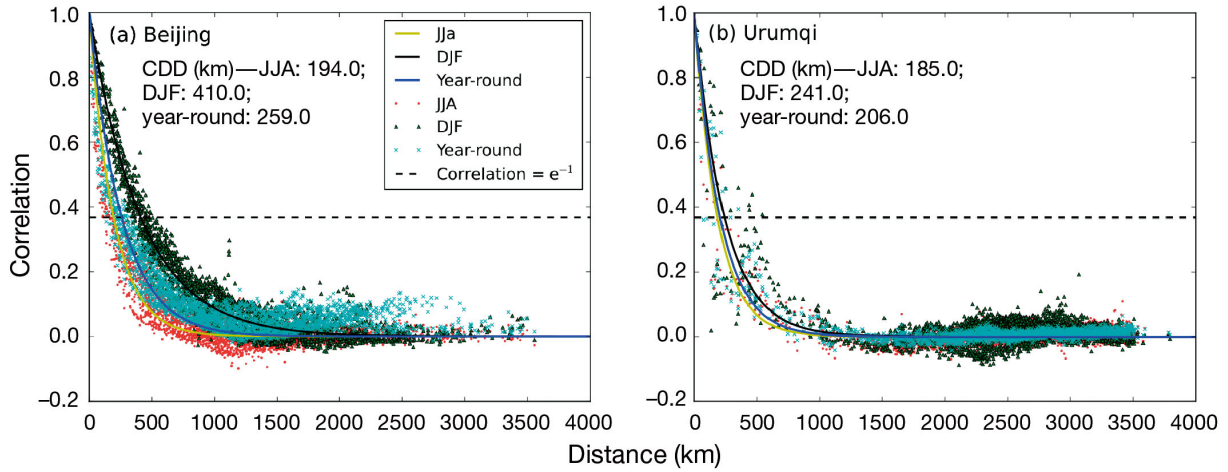


Fig. 3. Correlation decay distance (CDD, in km) at (a) Beijing station: 194.0 km using summer (JJA), 410.0 km for winter (DJF), and 259.0 km using year-round (annual) daily rainfall series, and (b) Urumqi station: 185.0, 241.0, and 206.0 km, respectively

whole of China, which may lead to some uncertainties in the correction factors. However, according to the results from Yang et al. (1991) and Sun et al. (2013), the difference of correction factors for snowfall in different areas is quite small, compared with the adjustment caused by bias correction. According to Goodison et al. (1998), the large differences in precipitation bias correction methods comes from various gauge types used in different countries, whereas all observations in China use the same Chinese standard gauge. It is very difficult to estimate the daily evaporation losses at regional station networks by using the average evaporation amount obtained from other experimental sites (Ye et al. 2004). Therefore, wetting losses, trace precipitation, and wind-induced gauge undercatch were corrected, while the evaporation loss was not corrected in this study.

4. VARIABILITY AND ANISOTROPY IN CDD

4.1. Comparison of year-round and seasonal CDDs at individual stations

We calculate CDDs not only using year-round daily rainfall, but also separately for 4 seasons (winter: DJF, spring: MAM, summer: JJA, and autumn: SON). Fig. 3 presents an example for stations in Beijing (39.80° N, 116.47° E) and Urumqi (43.78° N, 87.65° E). From Fig. 3, CDDs have a common feature, being shortest in JJA, and longest in DJF. The CDDs in MAM and SON are between those in JJA and DJF (not shown). This is expected owing to smaller-scale atmospheric features (e.g. convective rainfall system)

in JJA and larger-scale atmospheric systems (e.g. frontal rainfall system) in DJF. Also note the spatial differences in CDDs, with different stations presenting significantly different values in the same seasons (e.g. Beijing has a CDD of 410 km in DJF, 169 km more than that for Urumqi).

4.2. Geographical variations in CDD

CDDs based on year-round daily rainfall series show major geographical variations: they are shorter (<200 km) in Xinjiang Autonomous Region (XJ in Fig. 1c), the southwestern part of the Tibetan plateau (XZ in Fig. 1c), Sichuan basin (SC in Fig. 1c), and Hainan province (HI in Fig. 1c), and longer (>300 km) in northeastern China, and western China apart from Xinjiang (Fig. 4a). The short CDDs in Hainan probably result from tropical convective rainfall. Local geographical features may be the reason for short CDDs in other areas. Orographic rain caused by cold air from the northwest ascending the windward slope of the Tibetan massif, and a mosaic of mountains and deserts, may be the major reasons for the short CDDs in Xinjiang, and likewise for the southwestern border of the Tibetan plateau with warm moist air coming from the southwest. Additionally, the Tibetan plateau acts as a barrier to frontal influence. The Sichuan basin also has its own rainfall type due to its depressed orography. CDDs in winter are significantly larger than those in summer (Fig. 4b,d,f) owing to the different rainfall types: frontal in winter and convective in summer. Except for the Tibetan plateau and parts of northeastern

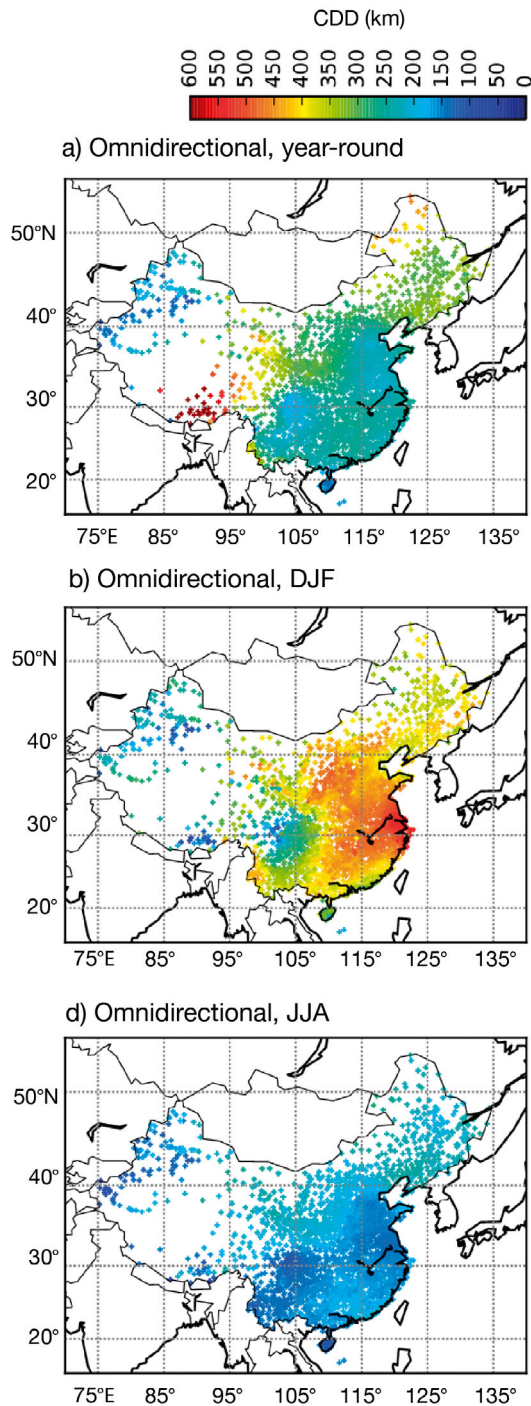
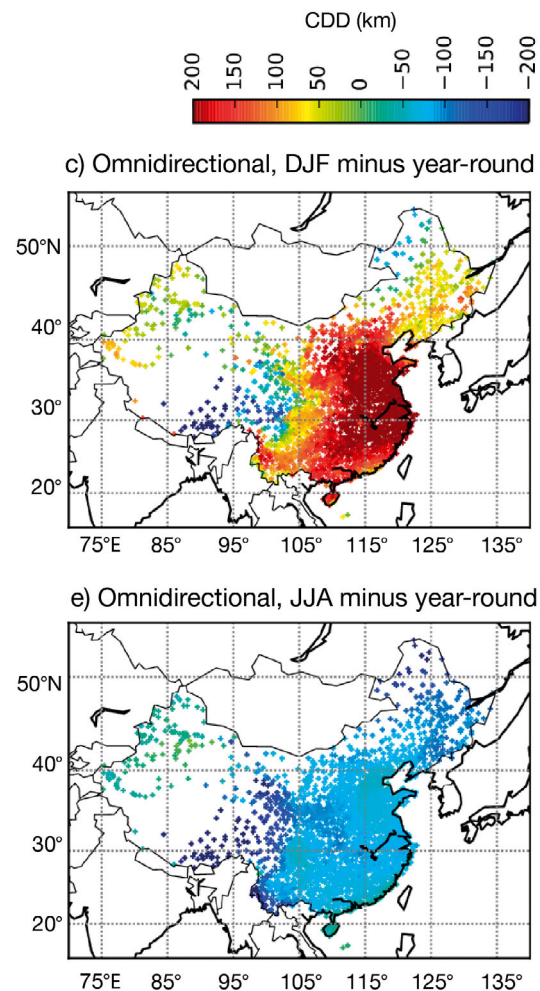


Fig. 4. Spatial patterns of correlation decay distance (CDD) of daily precipitation over mainland China for omnidirectional (a) year-round, (b) winter, (c) winter minus year-round, (d) summer, (e) summer minus year-round, (f) winter minus summer, and (g) year-round zonal, (h) year-round zonal minus omnidirectional, (i) year-round meridional, (j) year-round meridional minus omnidirectional, (k) year-round zonal minus meridional (figure continued on next page)

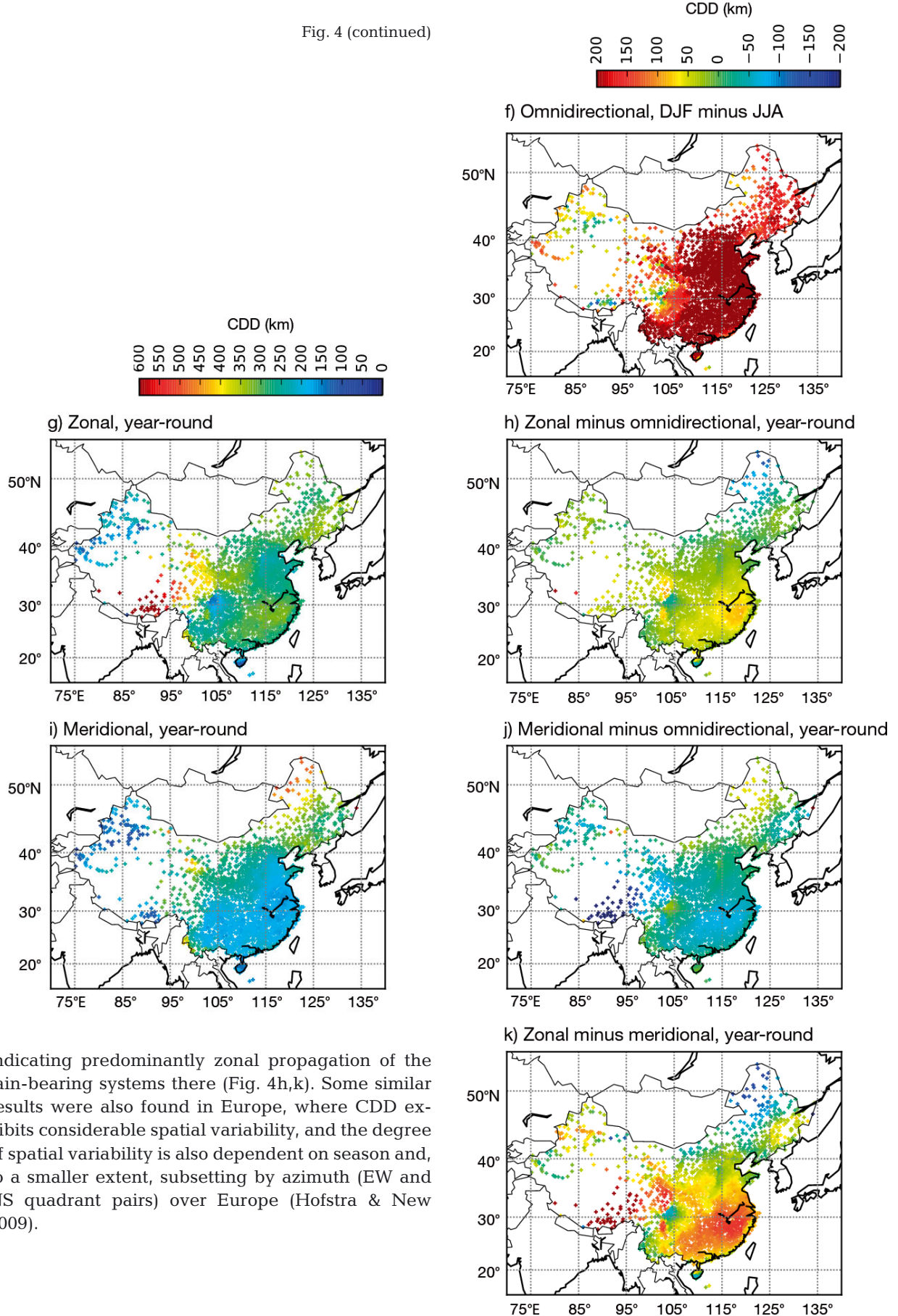


China, CDDs in winter are longer than those based on year-round daily data (Fig. 4c). CDDs for summer data are significantly smaller than for year-round data (Fig. 4e).

In order to estimate anisotropy in CDD, we calculated and compared zonal and meridional CDDs. To calculate meridional (zonal) CDD, only pairs of stations with relative angles of 0° (90°) from north, with 45° of tolerance, were considered. Compared with

the seasonal differences of CDDs (Fig. 4c,e,f), the differences between zonal and meridional CDDs and overall CDDs (Fig. 4h,j,k) are not very distinct. In northeastern China, meridional CDDs tend to be longer than zonal CDDs (Fig. 4k), probably owing to the nearly meridional propagation of frontal systems in winter. However, in most of southeastern China and the Tibetan plateau, zonal CDDs tend to be longer than overall CDDs and meridional CDDs,

Fig. 4 (continued)



5. EFFECT OF CORRELATION DECAY DISTANCE ON ANGULAR-DISTANCE WEIGHTING

In order to test the sensitivity of ADW interpolation skill to the assumptions made about CDD, we created alternative analyses using different CDDs, including a constant value of 258.45 km, which is the average of all CDDs based on year-round data for all of China (ADWc); omnidirectional CDD calculated using year-round daily data for the region applicable to each station (ADWr); omnidirectional CDD calculated by region and season (ADWr_s); and anisotropic CDD calculated by region and season (ADWr_{sa}). To combine zonal and meridional CDD for ADWr_{sa}, we applied an elliptical transformation, with the zonal and meridional CDDs as the axes of the ellipse. The equation of the ellipse is:

$$\left(\frac{x}{\text{CDD}_z}\right)^2 + \left(\frac{y}{\text{CDD}_m}\right)^2 = 1 \quad (5)$$

where x and y are Cartesian values correspondent to CDD for a given angle θ , which is the direction from one station to the target point (zero is towards the north, 90° is towards the east, etc.), and CDD_z and CDD_m are the zonal and meridional CDDs, respectively. Translating x and y into polar coordinates:

$$\begin{aligned} x &= \text{CDD} \sin \theta \\ x &= \text{CDD} \cos \theta \end{aligned} \quad (6)$$

Then:

$$\text{CDD} = \frac{1}{\sqrt{\left(\frac{\sin \theta}{\text{CDD}_z}\right)^2 + \left(\frac{\cos \theta}{\text{CDD}_m}\right)^2}} \quad (7)$$

Like Hofstra & New (2009), we chose 5 metrics to evaluate interpolation estimations: Pearson correlation (R), mean absolute error (MAE), compound relative error (CRE), proportion correct (PC), and critical success index (CSI). R, MAE, and CRE are used for evaluating the magnitude of estimated daily precipitation, whereas PC and CSI assess the daily rainfall state (wet or dry). The optimal metrics are 1 for R, PC, and CSI, and 0 for MAE and CRE.

R shows the linear relationship between 2 samples. Though R is insensitive to biases and errors in variance, it highlights the variations of the difference between predictions and observations (Murphy & Epstein 1989, Wilks 2006, Hofstra & New 2009):

$$R = \frac{C_{po}}{\sqrt{C_{pp} * C_{oo}}} \quad (8)$$

where C_{po} is the covariance of the predicted series p and the observation series o , and C_{pp} and C_{oo} are the variances of p and o , respectively.

MAE measures how close predictions are to real outcomes on average, and shows the errors in the same unit as the climate variable itself:

$$\text{MAE} = \frac{\sum_{k=1}^n |p_k - o_k|}{n} \quad (9)$$

where k is a particular station, p_k is the predicted series, o_k the observation series, and n the total pairs of stations.

CRE is a measure of similarity between predictions and observations (Murphy & Epstein 1989, Schmidli et al. 2001, Hofstra & New 2009):

$$\text{CRE} = \frac{\sum_{k=1}^n (p_k - o_k)^2}{\sum_{k=1}^n (o_k - \bar{o})^2} \quad (10)$$

where \bar{o} is the mean of the observation series, and n the total number of stations.

PC is defined as the number of correct categorizations divided by the total number of predictions (Hofstra & New 2009):

$$\text{PC} = \frac{w_c + d_c}{n} \quad (11)$$

where w_c and d_c are the number of correctly predicted wet and dry events, respectively, and n the total number of stations.

CSI also assesses categorization, and it is more appropriate than PC when one category is much more common than the other (Wilks 2006, Hofstra & New 2009):

$$\text{CSI} = \frac{w_c}{w_c + w_i + d_i} \quad (12)$$

where w_i and d_i are the numbers of incorrectly estimated wet events and dry events, respectively.

We use 191 of 213 RBSN gauges (Fig. 1b) for cross-validation. Twenty-two RBSN stations were rejected because they had too few data available to calculate climatology, or because they had too few neighbors within the CDD. Following previous research (e.g. Shen & Xiong 2016), we interpolate daily fractions (%) of the climatological average precipitation for the relevant month. This process reduces the influence of factors such as elevation and geography on the interpolation. The interpolated fractions are finally multiplied by the climatological average to yield actual precipitation. During cross-validation, each selected station is removed from the dataset in turn, and its daily rainfall anomalies (daily rainfall amount minus the monthly climatology) in 2008—when an extremely intense snowfall and freezing weather event (January and February) occurred in central and southern China—are estimated using the remaining stations. The predicted daily anomalies are multiplied by climatology to get the final estimated daily

rainfall series. Then the 5 metrics mentioned above (R, PC, CSI, MAE, and CRE) are used to evaluate the characteristics of the interpolated daily series over China as a whole (Table 1). On average, ADWr shows better scores for daily rainfall magnitude (MAE and CRE) than ADWc, with equal scores for daily rainfall state (PC and CSI). ADWr and ADWr_s show better scores than ADWc and ADWr for all metrics. ADWr_s is as good as ADWr for R and CRE, and better than ADWr for MAE, PC, and CSI. So allowing CDDs to vary spatially and seasonally improves the average ADW interpolation skills to some extent, and adding anisotropy appears to yield further improvement for China as a whole.

The differences are small, so we used standard errors (SEs) to assess the difference in metrics for different ADW versions (Fig. 5). Nearly all the SEs are less than half the margin of improvement (higher R, PC, CSI; lower MAE, CRE: Table 1) of ADWr_s relative to each other method. So allowing anisotropic CDDs to vary spatially and seasonally emerges as the best option.

To select the best interpolation skill for each region of China, we first rank the validation-station-average skill scores for a given metric for the 4 ADW versions in a given WMO block (e.g. Block 50 in northeastern China), then take the 5-metric average of these ranks in the block for a given ADW version, and finally rank these average ranks (Table 2). As well as doing this for the 10 WMO blocks, we also do it for 5

Table 1. All-China average skill scores for 4 versions of angular-distance weighting (ADW) for 191 Regional Basic Synoptic Network (RBSN) stations. Scores with underlines are optimal values. ADWc: average of all correlation decay distances (CDDs) based on year-round data for all of China, ADWr: omnidirectional CDD calculated using year-round daily data for the region applicable to each station, ADWr_s: omnidirectional CDD calculated by region and season, ADWr_sa: zonal and meridional CDD calculated by region and season, CRE: compound relative error, CSI: critical success index, MAE: mean absolute error, PC: proportion correct, R: Pearson correlation

ADW versions	R	MAE	CRE	PC	CSI
ADWc	0.783	1.612	0.414	0.849	0.586
ADWr	0.781	1.601	0.413	0.848	0.586
ADWr _s	<u>0.791</u>	1.563	<u>0.400</u>	0.853	0.593
ADWr _s a	<u>0.791</u>	<u>1.552</u>	<u>0.400</u>	<u>0.860</u>	<u>0.595</u>

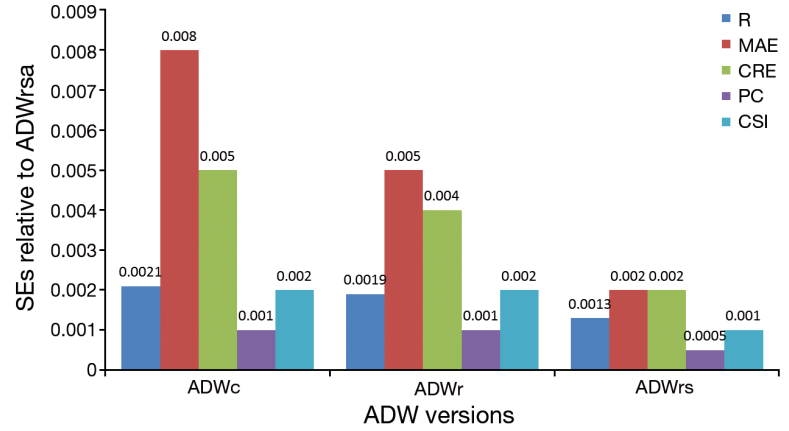


Fig. 5. Standard error (SE; standard deviation divided by square root of the number of validation stations) of all-China average skill scores of the angular-distance weighting (ADW) versions — ADWc: average of all correlation decay distances (CDDs) based on year-round data for all of China; ADWr: omnidirectional CDD calculated using year-round daily data for the region applicable to each station; ADWr_s: omnidirectional CDD calculated by region and season; ADWr_sa: the same as ADWr_s, but relative to zonal and meridional CDD. CRE: compound relative error; CSI: critical success index; MAE: mean absolute error; PC: proportion correct; R: Pearson correlation

regions (Cluster0 through Cluster4; Fig. 6) defined by *k*-means clustering of stations' 1981–2010 climatological average monthly precipitation (J. Hidalgo unpubl.) and smoothed to increase geographical coherence, as shown in Fig. 6b.

In densely monitored blocks (53, 54, 57, 58, and 59), ADWr_sa shows the best performance; therefore, anisotropic CDDs bring further benefit to ADW interpolation in dense observation networks. Addition-

Table 2. Regional ranks of skill for 4 different versions of angular-distance weighting (ADW), and Rank 1 with underlines are optimal choices. (2=) ADW versions are in the same rank. See Table 1 for ADW version abbreviations

WMO block or <i>k</i> -means cluster	No. of validation stations	ADWc	ADWr	ADWr _s	ADWr _s a
50	14	<u>1</u>	4	2	3
51	15	4	<u>1</u>	2	3
52	13	2=	4	<u>1</u>	2=
53	23	2	4	3	<u>1</u>
54	30	3	4	2	<u>1</u>
55	2	2	4	3	<u>1</u>
56	29	3	4	2	<u>1</u>
57	24	4	3	2	<u>1</u>
58	23	4	2	3	<u>1</u>
59	18	4	3	2	<u>1</u>
Cluster0	42	3	4	<u>1</u>	2
Cluster1	42	4	3	2	<u>1</u>
Cluster2	11	4	3	2	<u>1</u>
Cluster3	25	4	3	2	<u>1</u>
Cluster4	71	3	4	2	<u>1</u>

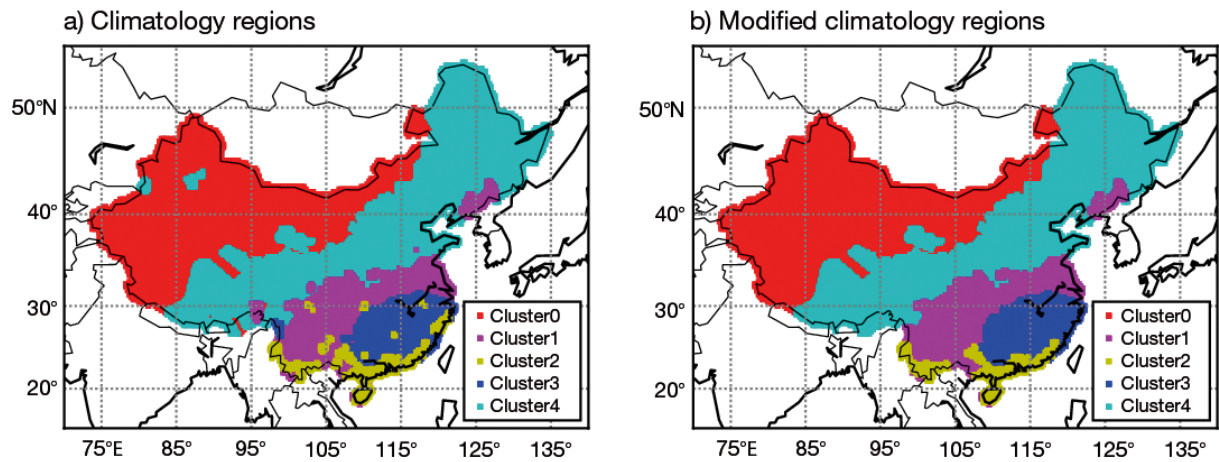


Fig. 6. Different climatology regions defined by 5-cluster k -means (J. Hidalgo unpubl.) that were (a) not modified, and (b) modified by adjusting some borderline or 'outlier' stations, interpolated to a 0.25 resolution grid. Each grid cell is assigned to the same cluster as the nearest station

ally, ADWr_{sa} is best in Block 55 where CDD is distinctly anisotropic (Fig. 4k). ADWr_{sa} also improves the interpolation skill in Block 56, where elevation varies between stations more than in the other blocks, ranging from 138 to 4533 m. However, anisotropic CDDs bring no further improvement in sparsely observed blocks (Blocks 50, 51, and 52). In summary, ADWr_{sa} is better than ADWr_s in regions with dense networks or very irregular terrain, or with distinctly anisotropic CDDs, but not in sparsely monitored regions (Blocks 50, 51, and 52; Cluster0).

Fig. 7 gives the regional skill scores of the top-ranked technique indicated in Table 2. Except for MAE, the scores of the top-ranked techniques for a

given metric are not hugely different from the overall scores for the corresponding metrics in Table 1. Mean annual precipitation can be classified as (cf. Ye et al. 2004, their Fig. 8a): ≥ 1000 mm (Blocks 59, 58, 57; Cluster2, Cluster3, Cluster1); < 500 mm (Blocks 51, 52, 53, 55; Cluster0); and 500–1000 mm (Blocks 56, 54, 50; Cluster4). As expected, the MAE of the best overall technique in Fig. 7 is very sensitive to the mean precipitation of the region, being large in humid regions and small in arid regions where PC is also good. Both R and CRE tend to have higher scores in intermediate and humid regions. PC performs better than CSI in arid regions, but the reverse holds in wet regions.

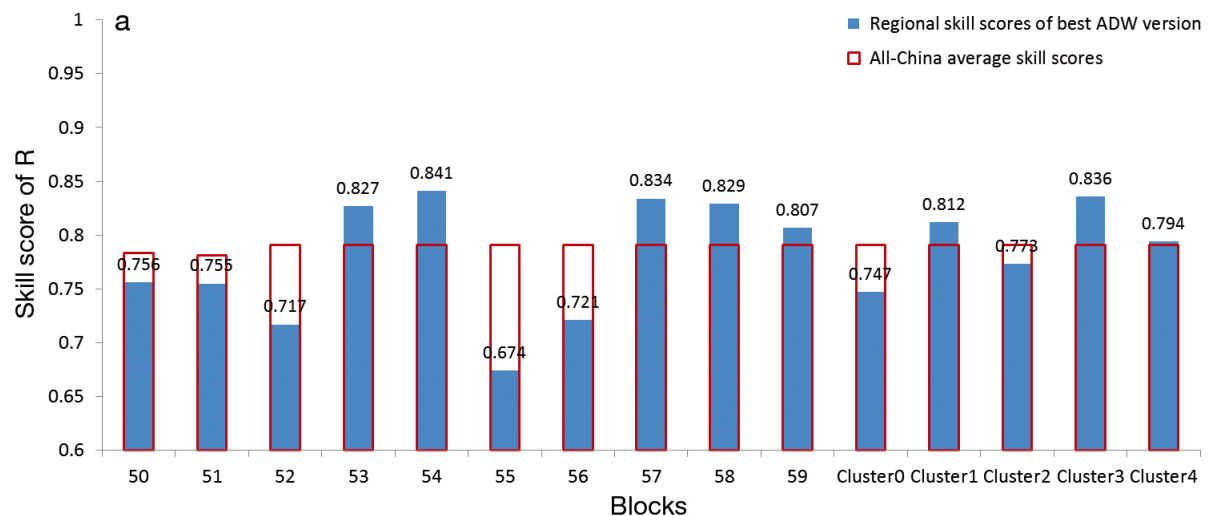


Fig. 7. Regional skill scores using the best overall angular-distance weighting (ADW) interpolation technique (blue bars), and overall scores for the same technique in Table 1 (red hollow bars) for (a) Pearson correlation (R), (b) mean absolute error (MAE), (c) compound relative error (CRE), (d) proportion correct (PC), and (e) critical success index (CSI) (figure continued on next page)

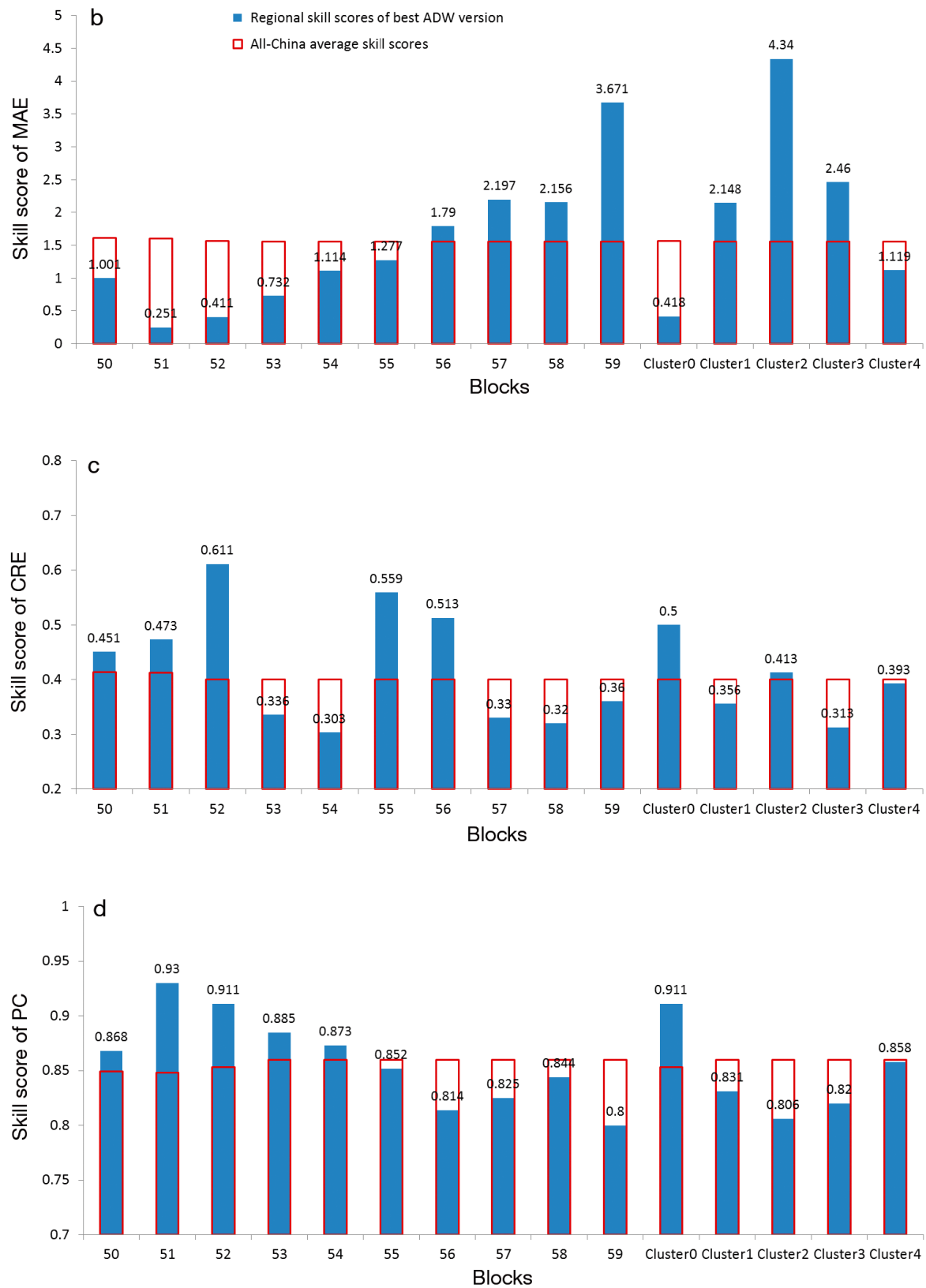


Fig. 7 (continued here and on next page)

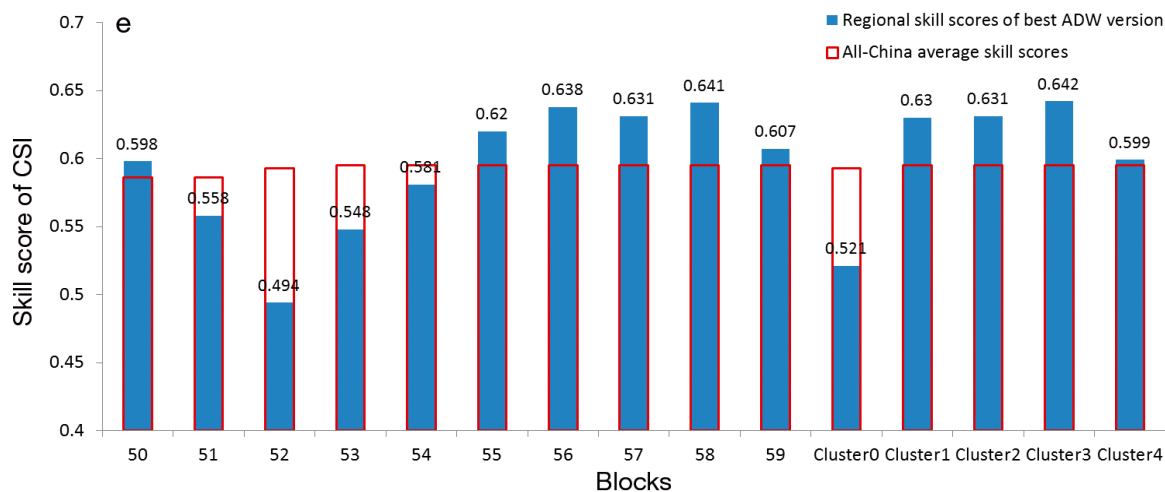


Fig. 7 (continued)

6. DISCUSSION AND CONCLUSIONS

We have found that for ADW interpolation, choosing a suitable CDD is the key factor, not only as the search radius for selecting appropriate stations, but also to calculate their respective weights more accurately. Variable (across space and time) CDDs have been widely used in the research community when interpolating fields such as precipitation and temperature using ADW. Taking this into account, we investigated the spatial and seasonal variability patterns of CDD of daily rainfall over mainland China. Additionally, an anisotropy analysis was carried out to consider possible directional effects. To evaluate the impact of these differences in CDDs on the ADW interpolation, we conducted a cross-validation exercise interpolating daily rainfall during 2008 using the different approaches.

We found that CDDs are shortest in JJA and longest in DJF over much of China. This is similar to the results in some other regions (e.g. Europe in Hofstra & New 2009), and is expected, owing to the smaller-scale atmospheric circulation and convective activity in JJA and the larger-scale atmospheric features and frontal activity in DJF. However, we also found some exceptions. In particular, some stations on the Tibetan plateau have unique characteristics owing to their special geography and topography (Fig. 4f,k). Compared with the seasonal differences of CDDs, the differences between anisotropic and isotropic CDDs are small. Places where meridional CDDs tend to be longer than zonal CDDs are likely to be dominated by nearly meridional rain-bearing systems, and vice versa.

From the cross-validation exercise, it can be concluded that, in general, when geographical and sea-

sonal varying effects are considered in CDD calculation, results improve in comparison with using a universal CDD. Further improvements in ADW interpolation are also achieved when anisotropy is included in the CDD calculation. These results are consistent across most of China (with the exception of less densely monitored areas in northwestern and northeastern China, where the rain gauge density is beneath 3 gauges per 1° latitude \times 1° longitude grid box). Anisotropic CDDs generally yield further improvement in regions with dense monitoring networks, very irregular terrain (southwestern China), or that have markedly anisotropic CDDs (Tibetan plateau).

Finally, from the results derived from our analysis, it can be concluded that it is advisable to take into account geographical, seasonal, and anisotropic effects when calculating and choosing CDDs. Our metrics for the chosen ADW schemes provide only parametric uncertainties, because they are related to the choices of CDD in ADW; future plans include a similar analysis using different interpolation techniques, such as kriging, in order to establish comparisons between different techniques and estimate structural uncertainties in the interpolation of daily precipitation over China.

Acknowledgements. This work and its contributors (Y.Z., J.H., D.P.) were jointly supported by the Special Scientific Research Fund of Meteorological Public Welfare Profession of China (Grant No. GYHY201406017), China Meteorological Administration Special Foundation for Climate Change (Grant No. CCSF201701, CCSF201702), National Key R&D Program of China (Grant No. 2016YFA0600301), and UK-China Research & Innovation Partnership Fund through the Met Office Climate Science for Service Partnership (CSSP) China as part of the Newton Fund.

LITERATURE CITED

- ✈ Alexander LV, Zhang X, Peterson TC, Caesar J and others (2006) Global observed changes in daily climate extremes of temperature and precipitation. *J Geophys Res* 111:D05109
- ✈ Briffa KR, Jones PD (1993) Global surface air temperature variations during the twentieth century. 2. Implications for large-scale high-frequency paleoclimatic studies. *Holocene* 3:77–88
- ✈ Brunsdon C, Fotheringham S, Charlton M (1998) Geographically weighted regression—modelling spatial non-stationarity. *J R Stat Soc D* 47:431–443
- ✈ Efthymiadis D, Jones PD, Briffa KR, Auer I and others (2006) Construction of a 10-min-gridded precipitation data set for the Greater Alpine Region for 1800–2003. *J Geophys Res* 111:D011505
- Goodison BE, Louie PYT, Yang D (1998) WMO solid precipitation measurement intercomparison: final report. WMO Tech Doc 872. WMO, Geneva, p 61–75
- ✈ Herrera S, Gutiérrez JM, Ancell R, Pons MR, Frías MD, Fernández J (2012) Development and analysis of a 50-year high-resolution daily gridded precipitation dataset over Spain (Spain02). *Int J Climatol* 32:74–85
- ✈ Hofstra N, New M (2009) Spatial variability in correlation decay distance and influence on angular-distance weighting interpolation of daily precipitation over Europe. *Int J Climatol* 29:1872–1880
- ✈ Jones PD, Osborn TJ, Briffa KR (1997) Estimating sampling errors in large-scale temperature averages. *J Clim* 10: 2548–2568
- ✈ Kiktev D, Sexton DMH, Alexander L, Folland CK (2003) Comparison of modeled and observed trends in indices of daily climate extremes. *J Clim* 16:3560–3571
- Korzun VI, Sokolow AA, Budyko MI, Voskresensky KP and others (1978) World water balance and water resources of the earth. Studies and reports in hydrology, No. 25. UNESCO, Paris
- ✈ Kuglitsch FG, Toreti A, Xoplaki E, Della-Marta PM, Luterbacher J, Wanner H (2009) Homogenization of daily maximum temperature series in the Mediterranean. *J Geophys Res* 114:D15108
- ✈ Legates DR, Willmott CJ (1990a) Mean seasonal and spatial variability in gauge-corrected global precipitation. *Int J Climatol* 10:111–127
- ✈ Legates DR, Willmott CJ (1990b) Mean seasonal and spatial variability in global surface air temperature. *Theor Appl Climatol* 41:11–21
- ✈ Lu GY, Wong DW (2008) An adaptive inverse-distance weighting spatial interpolation technique. *Comput Geosci* 34:1044–1055
- ✈ Murphy AH, Epstein ES (1989) Skill scores and correlation coefficients in model verification. *Mon Weather Rev* 117: 572–581
- ✈ New M, Hulme M, Jones PD (2000) Representing twentieth-century space-time climate variability. II. Development of 1901–1996 monthly grids of terrestrial surface climate. *J Clim* 13:2217–2238
- ✈ Osborn TJ, Hulme M (1997) Development of a relationship between station and grid-box rainfall frequencies for climate model evaluation. *J Clim* 10:1885–1908
- ✈ Schmidli J, Frei C, Schär C (2001) Reconstruction of meso-scale precipitation fields from sparse observations in complex terrain. *J Clim* 14:3289–3306
- Sevruk B, Hamon WR (1984) International comparison of national precipitation gauges with a reference pit gauge. In: WMO Instrum Obs Meth Rep No. 17. WMO, Geneva, p 1–111
- ✈ Shen Y, Xiong A (2016) Validation and comparison of a new gauge-based precipitation analysis over mainland China. *Int J Climatol* 36:252–265
- Shen Y, Feng MN, Zhang HZ, Gao F (2010) Research into daily precipitation interpolation methods over China. *J Appl Meteorol Sci* 21:279–286 (in Chinese)
- Shepard D (1968) A two-dimensional interpolation function for irregular-spaced data. In: Proc 23rd Assoc Computing Machinery (ACM) Natl Conf ACM New York, New York, NY, p 517–524
- Shepard D (1984) Computer mapping: the SYMAP interpolation algorithm. In: Gaile GL, Willmott CJ (eds) Spatial statistics and models. D Reidel Publishing, Dordrecht, p 133–145
- Sun X, Ren G, Ren Z, Shen Z (2013) Effects of wind-induced errors on winter snowfall and its trends. *Clim Environ Res* 18:178–186 (in Chinese)
- Wilks DS (2006) Statistical methods in the atmospheric sciences. In: Dmowska R, Hartmann D, Rossby HT (eds) *Int Geophys Ser*, Vol 91, 2nd edn. Academic Press, Burlington
- ✈ Willmott CJ, Rowe CM, Philpot WD (1985) Small-scale climate maps: a sensitivity analysis of some common assumptions associated with grid-point interpolation and contouring. *Am Cartogr* 12:5–16
- ✈ Xie P, Yatagai A, Chen M, Yatagai A and others (2007) A gauge-based analysis of daily precipitation over East Asia. *J Hydrometeorol* 8:607–626
- Yang D (1988) Research on analysis and correction of systematic errors in precipitation measurement in Urumqi River Basin, Tianshan. PhD dissertation, Lanzhou Institute of Glaciology and Geocryology, Chinese Academy of Sciences (in Chinese)
- Yang D, Shi Y, Kang E, Zhang Y, Yang X (1991) Results of solid precipitation measurement intercomparison in the Alpine area of Urumqi River basin. *Chin Sci Bull* 36: 1105–1109
- ✈ Yang D, Goodison BE, Metcalfe JR, Louie PYT and others (2001) Compatibility evaluation of national precipitation gauge measurements. *J Geophys Res* 106:1481–1492
- ✈ Ye B, Yang D, Ding Y, Han T, Koike T (2004) A bias-corrected precipitation climatology for China. *J Hydrometeorol* 5:1147–1160
- ✈ Yin H, Donat MG, Alexander LV, Sun Y (2015) Multi-dataset comparison of gridded observed temperature and precipitation extremes over China. *Int J Climatol* 35: 2809–2827
- ✈ Yuan W, Xu B, Chen Z, Xia J and others (2015) Validation of China-wide interpolated daily climate variables from 1960 to 2011. *Theor Appl Climatol* 119:689–700
- ✈ Zhou B, Xu Y, Wu J, Dong S, Shi Y (2016) Changes in temperature and precipitation extreme indices over China: analysis of a high-resolution grid dataset. *Int J Climatol* 36:1051–1066